Hittite Journal of Science and Engineering, 2022, 9 (1) 01–07
ISSN NUMBER: 2148–4171
DOI: 10.17350/HJSE19030000249

Selective Recognition of Kanamycin via Molecularly Imprinted Nanosensor

Esma Sari
Yuksek Ihtisas University, Department of Medical Laboratory Techniques, Ankara, Turkey

Article History:
Received: 2022/02/15
Accepted: 2022/02/28
Online: 2022/03/30

***Correspondence to**: Esra Sari,*
Yüksek Ihtisas University, Medical Laboratory Techniques, 06291, Ankara, Turkey.
E-Mail: esmasariuzek@yiu.edu.tr
Phone: +90 (312) 329 7425
Fax: +90 (312) 329 1421

ABSTRACT

Herein, the molecular recognition sites on the surface of the chip were created by the molecular imprinting method to produce the surface plasmon resonance (SPR) based nanosensor for the real-time kanamycin (KAN) detection. Firstly, kanamycin imprinted nanofilm, which has specific recognition cavities for kanamycin were synthesized by in-situ radical polymerization. Fabricated nanofilm for the detection of kanamycin was characterized with FTIR, ellipsometer, and atomic force microscope by the means of structurally and morphologically. The mean thickness values were determined for the imprinted and non-imprinted nanofilms as 102.4±3.1 nm and 101.8±4.7, respectively. The sensitivity performance of imprinted nanosensor was investigated by using the KAN solutions at different concentrations (25-200 ng/mL). The refractive index and the KAN concentration were found to be in perfect agreement with a regression coefficient (R^2, 0.992). The detection limit was calculated as 0.40±0.05 ng/mL by using the equation in the calibration curve. The response of imprinted and nonimprinted nanosensors towards the chemical analogs of KAN (NEO and SPM) were investigated to prove the selectivity of KAN imprinted nanosensors. The reusability performance of imprinted nanosensor was investigated by spiking 25 ng/mL KAN solution with three replicates. When the kinetic analyzes were examined, high sensitivity real-time kanamycin analysis was performed at very low concentrations with good reusability.

Keywords:
Kanamycin; Surface plasmon resonance; Molecular imprinting; Nanosensor.

INTRODUCTION

Kanamycin (KAN) indicates two forms of aminoglycoside, a crystalline monosulfate monohydrate, and salt with a higher sulfate content [1]. Due to their low cost of production, these compounds are widely used in the treatment of narrow therapeutic indexes, especially in veterinary medicine [2-5]. Despite its widespread use in the form of injections and capsules as a second-line antibiotic, there is increasing concern about KAN overuse, as well as overconsumption of KAN-containing animal-derived food because it could induce accumulation in an animal body and transferred into the food chain [3, 5, 6]. Residues of kanamycin were found to imperil people's health, causing severe side effects such as hearing loss, kidney damage, and allergic shock [3, 7]. In this sense, there are effective strategies accessible for kanamycin detection in various mediums. Until now, numerous analytical methods have been applied for the KAN detection such as spectrophotometry [3, 6], cantilever array sensor [5], high performance liquid chromatography (HPLC) [8, 9], solid-phase extraction (SPE) [9], electrochemical [4, 7, 10], mass spectrophotometry (MS) [9], capillary electrophoresis [11, 12]. While substantial contributions and recompensing results have been provided to the KAN detection, the majority of these methods are time-consuming, laborious, and complicated [2, 6, 7]. Furthermore, they often entail a significant amount of raw material, professional personnel, and costly equipment [2, 6, 10]. Therefore, rapid, simple, and low-cost methods for sensitive and selective KAN detection need to be developed. The molecular imprinting technique (MIT) is a powerful tool to create selective recognition regions on the surface of interest [7, 13-16]. There are many applications such as drug delivery [17], diagnostics [18], biosensors [19], forensic science [20], regenerative medicine [21], tissue engineering [22], etc. that is used effectively and successfully to obtain high sensitivity, specificity, and accuracy. Surface plasmon resonance (SPR) with undeniable advantages is a suitable platform to obtain a low detection limit for the sensing application of MIT [23-25]. The sensing system produced by the

combination of SPR and MIT is widely used in the detection of cells [20], pathogens [21, 26], biomolecules [27, 28], drugs [29], antibiotics [30-32], etc.

Herein, the nanosensor fabricated via MIT was developed to detect KAN with sensitivity and selectivity by using SPR. The KAN imprinted nanofilm which has specific recognition cavities for KAN were synthesized by in-situ radical polymerization on the chip surface. Before kinetic measurement of SPR chip surfaces with KAN imprinted nanofilms, FTIR, Ellipsometer, and AFM were used for the characterization of nanofilms on the surface of chips. The responses of nanosensors against KAN and competitors were investigated for selectivity studies. The KAN detection using the assay was successful, with high selectivity and sensitivity.

MATERIAL AND METHODS

Materials

Kanamycin (KAN), neomycin (NEO), spiramycin (SPM), allyl mercaptan, ethylene glycol dimethacrylate (EGDMA), methacrylic acid (MAA), and 2-hydroxyethyl methacrylate (HEMA), were obtained from Sigma Chemical Co (St. Louis, USA). Gold SPR chips were supplied from Horiba (UK). All other chemicals were of reagent grade and supplied from Sigma Chemical Co (St. Louis, USA) and Merck A.G (Darmstadt, Germany). All kinetic measurements were carried out with the SPR system (GenOptics, SPRi-Lab, Orsay, France). Barnstead D 3804 NANOpure cartridge with cellulose-containing Barnstead (Dubuque, A) RO pure LP reverse-osmosis unit was utilized for the purification of water used in all experiments.

Functionalization of the chip surface

The chip surface was functionalized with allyl mercaptan (CH_2CHCH_2SH). Before the modification, acidic piranha solution (3:1, H_2SO_4 / H_2O_2) was utilized to clean the gold surface. Then, ethyl alcohol was used as a washing solution for the cleaned chips, and the chips were placed to dry in a vacuum oven (200 mmHg, 40°C) for 3 hours. 10 µl of allyl mercaptan was applied to the cleaned SPR chip surface and allowed to stand for 12 hours. Following this, the final chips were washed with ethanol and dried in a nitrogen atmosphere. The modification resulted in the functionalization of the chip surface with allyl groups.

In situ synthesis of nanofilms

The following process was carried out for the fabrication of nanofilm on the surface of chips. The KAN selective molecularly imprinted nanofilm was obtained from the polymerization of MAA-KAN pre-complex towards EGDMA as a crosslinker and HEMA as a co-functional monomer. For the preparation of MAA-KAN pre-complex, 2 mg of KAN was complexed with 7.25 µL of MAA by providing a 1:5 (mmol) template molecule and functional monomer ratio. The pre-complex was dissolved by mixing 41 µL of toluene and 164 µL of ACN to obtain a homogeneous solution of the pre-complex. 13.4 µL of HEMA monomer and 27.7 µL of EGDMA crosslinker were added to the pre-complex solution. After adding AIBN (10 mg) as initiator, the final solution (5 µL) was dripped on the pre-vinylated chip. The prepared chip was placed under a UV lamp and polymerization was achieved by photopolymerization for 75 minutes. The unreacted monomer was removed with ethyl alcohol. The ratio of the crosslinker, monomer, and template molecule is 20:14:1, respectively. The percentage of monomer in solution was determined as 25 % (w/v). After the polymerization steps, the imprinted nanofilm-coated SPR chip was washed with methanol and acetonitrile solution (4:1, MeOH:MeCN) to extract the template. The KAN imprinted nanofilm was washed with this desorption solution at room temperature for one hour, renewing the desorption solution every ten minutes. This process was repeated until KAN could not be detected by UV spectrophotometer at 276 nm. To prove the selectivity of KAN imprinted nanofilm, the non-imprinted nanofilm was also fabricated in the same manner as described earlier without adding KAN.

Characterization of nanofilms

The thickness measurements on the surfaces of the prepared sensors were characterized by Nanofilm EP3-Nulling Ellipsometer (Göttingen, Germany). The laser with the wavelength of 532 nm at an incidence angle of 62° was used to perform thickness measurements. The SPR sensor is positioned beneath the laser light source. The average of the kinetic measurement results repeated three times in six different regions is reported. The contact angles of nanofilms were measured using a KRUSS DSA100 (Hamburg, Germany) instrument. The contact angles were determined by pouring water on the SPR chip surfaces using the Sessile Drop technique. For each drop, five independent photographs were taken from different regions of the chip surface to calculate contact angle data. Five independent photographs were recorded from various regions of the surface of the chips, and the contact angle data were calculated for each drop. The structural characterization of the nanofilm surfaces was carried out using Fourier transform infrared spectrometer (Thermo Fisher Scientific, Nicolet iS10, Waltham, MA, USA).

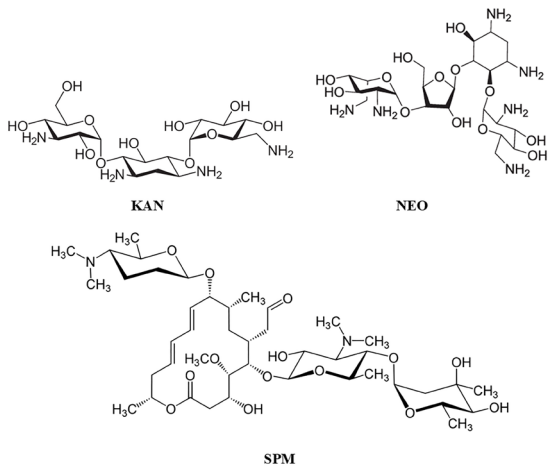

Figure 1. The molecular structures of KAN, NEO and SPM.

SPR measurement

Kinetic measurements by the KAN imprinted nanosensors were carried out by surface plasmon resonance. The kanamycin solutions at different concentrations (25-200 ng/mL) were interacted with SPR nanosensors by a peristaltic pump and kinetic data were obtained using SPRview software.

The following steps were applied for the real-time SPR analysis: first equilibrium buffer (Phosphate buffer, 10 mM, pH 7.5) then KAN solution was passed through the system until the system reached equilibrium again, and the desorption solution (2.0 M NaOH) was used in the last step. In all measurements, the equilibrium buffer waited for 5 minutes and kanamycin solution was waited for 10 minutes for the system to reach equilibrium. Desorption and regeneration processes were carried out in about 15 minutes. The isotherm models can be applied to examine the interaction between the imprinted nanosensor and KAN in the graphs. The response of imprinted and nonimprinted nanosensors towards the chemical analogs of KAN (NEO and SPM) were investigated to prove the selectivity of KAN imprinted nanosensors. The molecular structures of KAN, NEO and SPM were given in Figure 1. The reusability performance of imprinted nanosensor was investigated by spiking 25 ng/mL KAN solution with three cycles.

RESULTS AND DISCUSSION

Characterization

The average surface thickness of the nanofilm was investigated through spectroscopic ellipsometry. As seen in Figure 2, the mean thickness values were determined for the imprinted and non-imprinted nanofilms as 102.4±3.1 nm and 101.8±4.7, respectively.

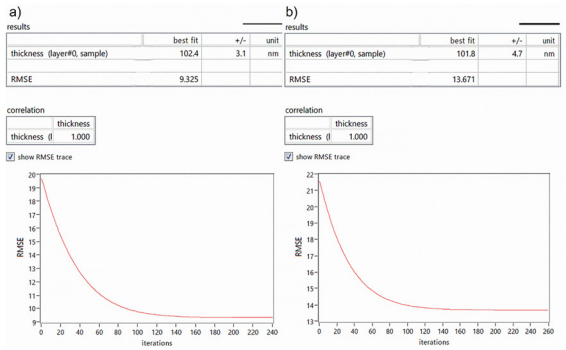

Figure 2. The molecular structures of KAN, NEO and SPM.

The surface hydrophobicity of the SPR chip surface was investigated by taking the contact angle measurements. The contact angles of imprinted, nonimprinted, and unmodified SPR chips were measured as 60.5°, 62.2°, and 76.4°, respectively (Figure 3). The decreasing of contact angle values indicates an increment in wettability as a result of the decrease in hydrophobicity. The imprinted and nonimprinted nanofilms synthesized on the chip surface have a hydrophilic character originating from the monomers (HEMA, EGDMA, and MAA) used, therefore, as expected, the contact angles are lower than the unmodified SPR chip.

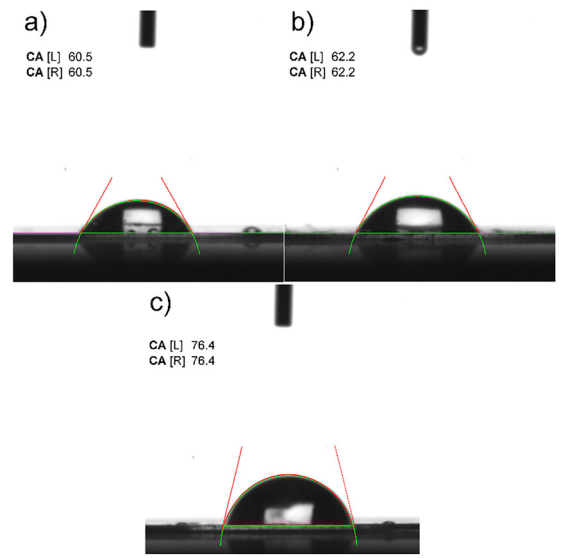

Figure 3. Contact angle measurement of SPR chips: imprinted (a), nonimprinted (b), and unmodified (c).

FTIR-ATR spectroscopy analysis was carried out for the structural characterization of nanofilms. The similarities in the chemical structures of nanofilms caused by crosslinker and functional monomers are clearly visible in FTIR-ATR spectra (Figure 4). The most prominent bands in the spectra, as shown in Figure 4, were O–H stretching bands, which correspond to the hydroxyl group of HEMA at about 3200–3300 cm^{-1}; aliphatic C–H stretching bands, which correspond to the methyl group of MAA and EGDMA at about 2900–3000 cm^{-1}; and C=O stretching bands,

which correspond to the carbonyl group of MAA, HEMA and EGDMA at about 1700–1750 cm^{-1}; aliphatic C–H bending bands corresponds to the methyl group of MAA and EGDMA at about 1400– 1500 cm^{-1}; C–O stretching bands corresponds to the carboxyl group of MAA, HEMA and EGDMA at about 1150–1250 cm^{-1}. These bands in both spectra demonstrated the presence of MAA and HEMA in the structure of nanofilms.

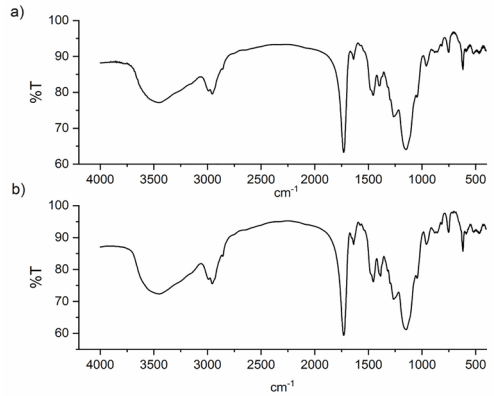

Figure 4. FTIR analysis of imprinted (imprinted) and nonimprinted (nonimprinted) nanofilms.

Kinetic and Equilibrium Analysis

To evaluate the relationship between SPR signal and kanamycin concentration, kanamycin solutions at various concentrations (25-200 ng/mL) were analyzed by the KAN imprinted nanosensor (Figure 5). The changes in the refractive index versus time were given in Figure 4a by applying the KAN solutions at the different concentrations to the imprinted nanosensors. As can be seen from the figures, the % refraction value increases with the application of kanamycin to the imprinted SPR nanosensor. The reason for this can be shown as the increase in the concentration difference, which is the driving force between the kanamycin solution and the surface. As seen in Figure 5, the % refraction value increases with the application of kanamycin to the surface. In a standard measurement; equilibrium solution was passed through the system first, then kanamycin solution until the system reached equilibrium again, and desorption solution was used in the last step. In all measurements, approximately 20 minutes were waited for the system to reach equilibrium. Desorption and regeneration processes were carried out in about 15 minutes. It was observed that the % refraction value increased greater with increasing the concentration. The reason for this can be explained as the increase in the concentration difference, which is the driving force between the KAN solution and the surface of imprinted nanofilm. The amount of KAN can be determined by using the calibration plot giving the relationship between SPR signal and KAN concentration in Figure 5b. The refractive index and the KAN concentration were found to be in perfect agreement (R2, 0.992). The detection limit was calculated as 0.40±0.05 ng/mL by using the calibration curve. When the kinetic analyzes were examined, high sensitivity real-time kanamycin analysis was performed at very low concentrations. Considering the importance of detecting residues of kanamycin for human health even at low concentrations, this method is thought to be a very successful technique for kanamycin analysis compared to literature (Table 1).

It is required to determine the binding parameters from the measurements of the process to quantify binding features. For the determination of constants, the models, whose equations are given below, are applied to the data [37-39].

$$Association\,kinetic\,analysis\;\frac{d\Delta R}{dt} = k_a C(\Delta R_{\max} - \Delta R) - k_d \Delta R \quad (1)$$

$$Scatchard\;\frac{\Delta R_{ex}}{[C]} = K_A(\Delta R_{\max} - \Delta R_{eq}) \quad (2)$$

$$Freundlich\;\Delta R = \Delta R_{\max}[C]^{\frac{1}{n}} \quad (3)$$

$$Langmuir\;\Delta R = \left[\frac{\Delta R_{\max}[C]}{K_d + [C]}\right] \quad (4)$$

$$Langmuir - Freundlich\;\Delta R = \left[\frac{\Delta R_{\max}[C]^{\frac{1}{n}}}{K_d + [C]^{\frac{1}{n}}}\right] \quad (5)$$

where dR/dt is the change of the refractive index in unit time, R and R_{max} are experimental sensor responses measured during analyte molecule binding (Reflectivity %/s) and theoretical maximum sensor response, C is the concentration (M), k_a is the association rate constant (L/mol.s), k_d is the dissociation rate constant (1/s), and 1/n is the Freundlich heterogeneity index. The association constant, K_a, can be computed as $K_a = k_a/k_d$ (L/mol), while the dissociation constant, K_d (mol/L), is equal to $1/K_a$.

Table 1. The comparison of studies for the detection of KAN in literature.

Technique	Method	LOD (nM)	[R]
SPR	Aptamer based sensing	285	31
SPR	Molecular imprinting	12	32
Colorimetric	Aptamer based sensing	25	33
Fluorometric	Oligonucleotide	0.37	34
Electrochemical	Aptamer based sensing	2.37	35
Colorimetric	Chitosan-wrapped gold nanoparticles	8.0	36
SPR	Molecular imprinting	0.8	This study

The rate and equilibrium parameters reveal the intensity of association and dissociation tendency for the interaction of surface and molecule. As shown in Table 2, the association rate constant and s for (k_a) and the dissociation rate constant (k_d) were calculated as $2.2x10^2$ $M.s^{-1}$ and $2.8x10^{-3}$ s^{-1}, respectively, while the association (K_a) and dissociation (K_d)

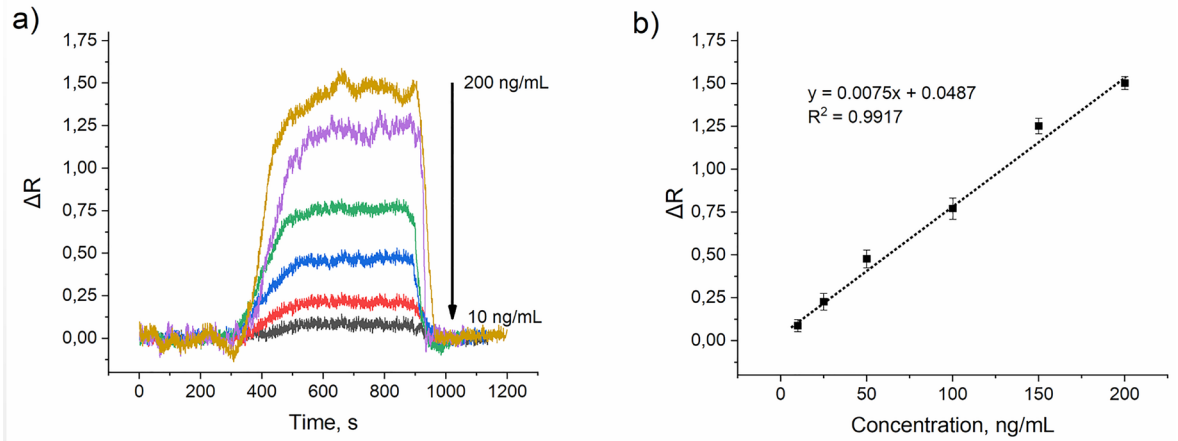

Figure 5. Real-time analysis of KAN with ERY via imprinted nanosensor: effect of concentration on the signal of imprinted SPR nanosensors (a) and the calibration curve obtained by plotting KAN concentration versus. ΔR (b).

Table 2. The comparison of studies for the detection of KAN in literature.

Association Analysis		Scatchard Analysis	
k_a ($M.s^{-1}$)	2.2×10^{2}	ΔR_{max}	9.78
k_d (s^{-1})	2.8×10^{-3}	K_a (M^{-1})	4.1×10^{5}
K_a (M^{-1})	7.7×10^{5}	K_d (M)	2.4×10^{-6}
K_d (M)	1.3×10^{-6}	R^2	0.607
R^2	0.9743		

Table 3. Isotherm parameters.

Freundlich		Langmuir		Langmuir-Freundlich	
ΔR_{max}	1.870	ΔR_{max}	2.508	ΔRmax	18.018
1/n	0.947	K_a (M^{-1})	7.40×10^{4}	1/n	0.947
R^2	0.996	K_d (M^{-1})	1.35×10^{-5}	Ka (M^{-1})	1.40×10^{4}
		R^2	0.958	Kd (M)	7.20×10^{-5}
				R^2	0.936

constants were 7.7×10^{5} M^{-1} and 1.3×10^{-6} M. As can be seen, the interactions between the nanosensor and KAN have a high affinity according to the association (K_a) and dissociation (K_d) constants.

Adsorption isotherm models were utilized to examine the surface heterogeneity and binding behaviours of imprinted nanosensors. The binding characteristics were investigated by using the Langmuir and Scatchard models for the imprinted nanosensor (Table 3). The Langmuir model supposes that the surface has homogeneous binding sites with the same binding affinity coefficient. The Freundlich model describes the heterogeneous binding behavior of surfaces. This model is useful for estimating adsorption on the heterogeneous nature of surfaces and thus avoiding the limitation of higher concentration related to the Freundlich model. Therefore, this model has been explained by Freundlich Isotherm at low concentration and the Langmuir model at high concentration.

The Freundlich model was used to match the experimental binding isotherms based on correlation coefficient and linearity data, as shown in Table 3. According to the Freundlich model, Rmax and the Freundlich constant, 1/n, were calculated to be 1.87 and 0.947, respectively. Although the binding sites on the kanamycin imprinted nanosensor are diverse, the population of high-affinity binding sites is greater. Consequently, the Freundlich model is best suited to elucidate the binding behaviors of imprinted polymers.

Selectivity of nanosensor

The response of imprinted and nonimprinted nanosensors towards the chemical analogs of KAN (NEO and SPM) were investigated to prove the selectivity of KAN imprinted nanosensors. The assay for the detection of KAN was separately applied to the chemical analogs solutions onto the imprinted and nonimprinted nanosensor and the sensograms are shown in Figure 6. As seen in Figure 6b, the nonimprinted nanosensor is non-selective and has a poor sensitivity to detect KAN. However, the imprinted nanosensor produces a strong signal with good selectivity for the detection of KAN (Figure 6a). The selectivity results prove that the imprinted nanofilm has specific cavities to recognize the KAN with high sensitivity and selectivity.

Reusability of nanosensor

The reusability performance of imprinted nanosensor was investigated by spiking 25 ng/mL KAN solution with three cycles. As seen in Figure 7, the change in the response of nanosensor after a three-cycle is not significant to detect kanamycin. Consequently, the developed nanosensor system indicates good repeatability to recognize kanamycin in an aqueous solution.

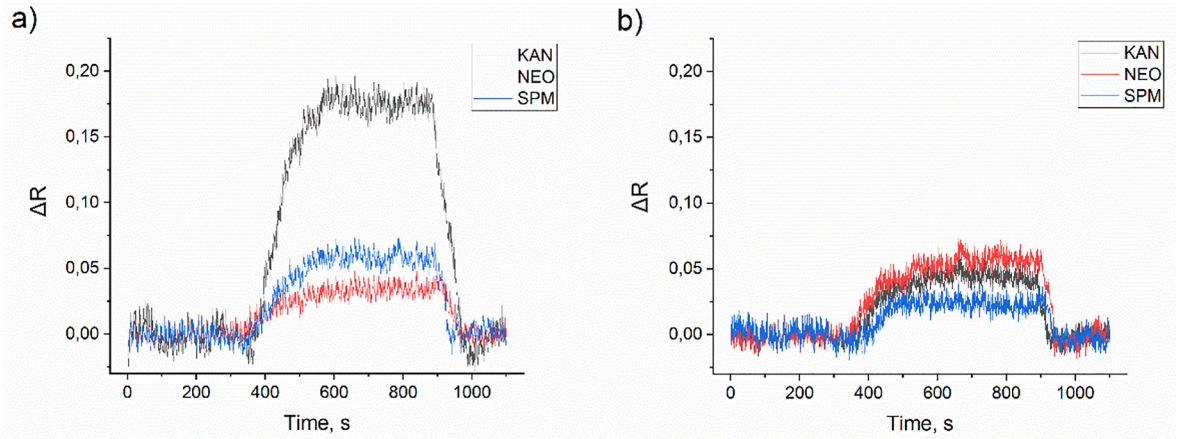

Figure 6. The SPR responses of imprinted (a) and nonimprinted (b) nanosensors for KAN, NEO, and SPM.

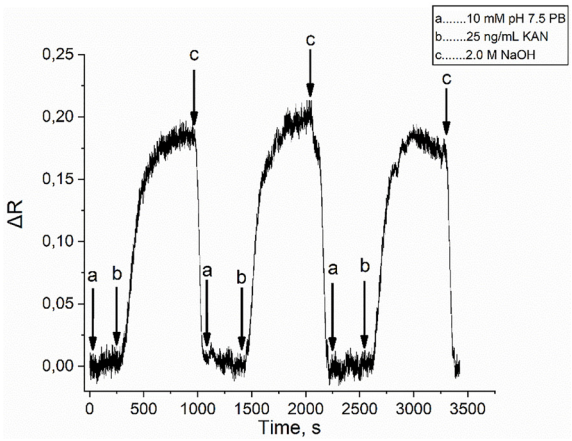

Figure 7. Reusability of the imprinted SPR nanosensor.

CONCLUSION

In this research, the KAN imprinted nanofilm for the SPR sensor was constructed and successfully synthesized by in-situ radical polymerization. Various methodologies were used to characterize the constructed system, and the refractive index changes were analyzed depending on the relation between the KAN concentrations and the signal enhancements. the refractive index changes depending on the relationship between kanamycin concentrations and signal enhancements were analyzed. The responses of imprinted nanosensors were found to be effective for detecting analytes of interest, whereas non-imprinted nanosensor responses were ineffective. For the detection of kanamycin, numerous analytical approaches have been used, including solid-phase extraction (SPE), spectrophotometry, electrochemical, high-performance liquid chromatography (HPLC), mass spectrophotometry (MS), cantilever array sensor, and capillary electrophoresis [3-12]. Such systems, in contrast to the suggested sensing system, are arduous, expensive, time-consuming, and difficult. Based on these findings, the imprinted nanosensors are capable of selectively capturing KAN from aqueous media. The imprinted nanofilms appear to be a promising tool for sensing applications in this area. Based on this successful approach and ease of extension to the analysis of additional analytes, the SPR system in combination with the MIP method is envisioned as a potential technique for detecting residues.

CONFLICT OF INTEREST

There is no financial conflict of interest with any institution, organization, person related to our article named "Selective Recognition of Kanamycin via Molecularly Imprinted Nanosensor" and there is no conflict of interest between the authors.

References

1. Claes PJ, Dubost M, Vanderhaeghe H. Kanamycin sulfate, Analytical Profiles of Drug Substances., New York, pp. 259–296, 1977.
2. Sharma N, Selvam SP, Yun K. Electrochemical detection of amikacin sulphate using reduced graphene oxide and silver nanoparticles nanocomposite. Applied Surface Science 512 (2020) 145742.
3. Xu Y, Han T, Li X, Sun L, Zhang Y, Zhang Y. Colorimetric detection of kanamycin based on analyte-protected silver nanoparticles and aptamer-selective sensing mechanism. Analytica Chimica Acta 891 (2015) 298-303.
4. Rahman M M. Chemical, Label-free Kanamycin sensor development based on CuONiO hollow-spheres: food samples analyses. Sensors and Actuators B: Chemical 264 (2018) 84-91.
5. Bai X, Hou H, Zhang B, Tang J. Label-free detection of kanamycin using aptamer-based cantilever array sensor. Biosensors and Bioelectronics 56 (2014) 112-116.
6. Wang R, Wang R, Ge B, Jia X, Li Z, Chang J. Spectral method determination of kanamycin sulfate using both gold nanoparticles and quantum dots. Analytical Methods 19 (2013) 5302-5308.
7. Long F, Zhang Z, Yang Z, Zeng J, Jiang Y. Imprinted electrochemical sensor based on magnetic multi-walled carbon nanotube for sensitive determination of kanamycin. Journal of Electroanalytical Chemistry 755 (2015) 7-14.
8. Adams E, Dalle J, De Bie E, De Smedt I, Roets E, Hoogmartens J. Analysis of kanamycin sulfate by liquid chromatography with

pulsed electrochemical detection. Journal of Chromatography A 766 (1997) 133-139.
9. Tao Y, Chen D, Yu H, Huang L, Liu Z, Cao X, Yan C, Pan Y, Liu Z, Yuan Z. Simultaneous determination of 15 aminoglycoside (s) residues in animal derived foods by automated solid-phase extraction and liquid chromatography–tandem mass spectrometry. Food Chemistry 135 (2012) 676-683.
10. Song HY, Kang TF, Li NN, Lu LP, Cheng SY. Highly sensitive voltammetric determination of kanamycin based on aptamer sensor for signal amplification. Analytical Methods 16 (2016) 3366-3372.
11. Lin YF, Wang YC, Chang SY. Capillary electrophoresis of aminoglycosides with argon-ion laser-induced fluorescence detection. Journal of Chromatography A 1188 (2008) 331-333.
12. Kaale E, Van Schepdael A, Roets E, Hoogmartens J. Development and validation of a simple capillary zone electrophoresis method for the analysis of kanamycin sulfate with UV detection after pre-capillary derivatization. Journal of Chromatography A 924 (2001) 451-458.
13. Arabi M, Ostovan A, Li J, Wang X, Zhang Z, Choo J, Chen L. Molecular imprinting: green perspectives and strategies. Advanced Materials 33 (2021) 2100543.
14. Mosbach K. Molecular imprinting. Trends in biochemical sciences 19 (1994) 9-14.
15. Mosbach K, Ramström O. The emerging technique of molecular imprinting and its future impact on biotechnology. Bio/technology 14 (1996) 163-170.
16. Wulff G. Molecular imprinting in cross-linked materials with the aid of molecular templates—a way towards artificial antibodies. Angewandte Chemie International Edition in English 34 (1995) 1812-1832.
17. He S, Zhang L, Bai S, Yang H, Cui Z, Zhang X, Li Y. Advances of molecularly imprinted polymers (MIP) and the application in drug delivery. European Polymer Journal 143 (2021) 110179.
18. Piletsky SS, Piletska E, Poblocka M, Macip S, Jones DJL, Braga M, Cao TH, Singh R, Spivey AC, Aboagye EO, Piletsky SA. Snapshot imprinting: rapid identification of cancer cell surface proteins and epitopes using molecularly imprinted polymers. Nano Today 41 (2021) 101304.
19. Zhang J, Wang Y, Lu X. Molecular imprinting technology for sensing foodborne pathogenic bacteria. Analytical and Bioanalytical Chemistry 413 (2021) 4581-4598.
20. Balayan S, Chauhan N, Chandra R, Jain U. Molecular imprinting based electrochemical biosensor for identification of serum amyloid A (SAA), a neonatal sepsis biomarker. International Journal of Biological Macromolecules 195 (2022) 589-597.
21. Perez-Puyana V, Wieringa P, Guerrero A, Romero A, Moroni L. (Macro) Molecular Imprinting of Proteins on PCL Electrospun Scaffolds. ACS Applied Materials & Interfaces 13.25 (2021) 29293-29302.
22. Bonatti AF, De Maria C, Vozzi G. Molecular imprinting strategies for tissue engineering applications: A review. Polymers 13 (2021) 548.
23. Cennamo N, D'Agostino G, Pesavento M, Zeni L. High selectivity and sensitivity sensor based on MIP and SPR in tapered plastic optical fibers for the detection of L-nicotine. Sensors and Actuators B: Chemical 191 (2014) 529-536.
24. Matsui J, Akamatsu K, Hara N, Miyoshi D, Nawafune H, Tamaki K, Sugimoto N. SPR sensor chip for detection of small molecules using molecularly imprinted polymer with embedded gold nanoparticles. Analytical Chemistry 77 (2005) 4282-4285.
25. Shrivastav AM, Mishra SK, Gupta BD. Fiber optic SPR sensor for the detection of melamine using molecular imprinting. Sensors and Actuators B: Chemical 212 (2015) 404-410.
26. Meneghello A, Sonato A, Ruffato G, Zacco G, Romanato F. A novel high sensitive surface plasmon resonance Legionella pneumophila sensing platform. Sensors and Actuators B: Chemical 250 (2017) 351-355.
27. Bognár Z, Supala E, Yarman A, Zhang X, Bier FF, Scheller FW, Gyurcsányi RE. Peptide epitope-imprinted polymer microarrays for selective protein recognition. Application for SARS-CoV-2 RBD protein. Chemical Science 13 (2022) 1263-1269.
28. Sinha RK. Wavelength modulation based surface plasmon resonance sensor for detection of cardiac marker proteins troponin I and troponin T. Sensors and Actuators A: Physical 332 (2021) 113104.
29. Jagirani MS, Mahesar SA, Uddin S, Sherazi STH, Kori AH, Lakho SA, Kalwar NH, Memon SS. Functionalized Gold Nanoparticles Based Optical, Surface Plasmon Resonance-Based Sensor for the Direct Determination of Mitoxantrone Anti-cancer Agent from Real Samples. Journal of Cluster Science 33 (2022) 241-247.
30. Wang W, Wang R, Liao M, Kidd MT, Li Y. Rapid detection of enrofloxacin using a localized surface plasmon resonance sensor based on polydopamine molecular imprinted recognition polymer. Journal of Food Measurement and Characterization 15 (2021) 3376-3386.
31. Écija-Arenas Á, Kirchner EM, Hirsch T, Fernández-Romero, JM. Development of an aptamer-based SPR-biosensor for the determination of kanamycin residues in foods. Analytica Chimica Acta 1169 (2021) 338631.
32. Zhang L, Zhu C, Chen C, Zhu S, Zhou J, Wang M, Shang P. Determination of kanamycin using a molecularly imprinted SPR sensor. Food chemistry 266 (2018) 170-174.
33. Song KM, Cho M, Jo H, Min K, Jeon SH, Kim T, Ban C. Gold nanoparticle-based colorimetric detection of kanamycin using a DNA aptamer. Analytical biochemistry 415 (2011) 175-181.
34. Zhu Y, Li W, Tan S, Chen TA. A label-free and functional fluorescent oligonucleotide probe based on a G-quadruplex molecular beacon for the detection of kanamycin. Chemical Research in Chinese Universities 34 (2018) 541-545.
35. Li F, Wang X, Sun X, Guo Y. An aptasensor with dsDNA for rapid and highly sensitive detection of kanamycin in milk. RSC advances 7 (2017) 38981-38988.
36. Lai C, Liu X, Qin L, Zhang C, Zeng G, Huang D, Huang D. Chitosan-wrapped gold nanoparticles for hydrogen-bonding recognition and colorimetric determination of the antibiotic kanamycin. Microchimica Acta 184 (2017) 2097-2105.
37. Sari E, Üzek R, Duman M, Denizli A. Detection of ciprofloxacin through surface plasmon resonance nanosensor with specific recognition sites. Journal of Biomaterials science, Polymer edition, 29 (2018) 1302-1318.
38. Sari E, Üzek R, Duman M, Denizli A. Fabrication of surface plasmon resonance nanosensor for the selective determination of erythromycin via molecular imprinted nanoparticles. Talanta 150 (2016) 607-614.
39. Sari E, Üzek R, Duman M, Alagöz HY, Denizli A. Prism coupler-based sensor system for simultaneous screening of synthetic glucocorticosteroid as doping control agent. Sensors and Actuators B: Chemical 260 (2018) 432-444.